



Preparation of Micro-porous Polyethersulphone Hollow Fibre Membranes Using Non-solvent Vapour-induced Phase Separation

Gui-E Chen^{1,2}, Jing-Feng Li², Ling-Feng Han², Zhen-Liang Xu^{2*},
and Li-Yun Yu²

(1) School of Chemical and Environmental Engineering,

Shanghai Institute of Technology, Shanghai 200233, P.R. China

(2) Membrane Science and Engineering R&D Lab, Chemical Engineering Research Center, East China University of Science and Technology, Shanghai 200237, P.R. China

Received 10 February 2010; accepted 20 September 2010

ABSTRACT

Using a dope comprised of polyethersulphone (PES):*N,N*-dimethylacetamide: diethylene glycol (DEG) 17:43:40 (wt%), micro-porous PES hollow fibre membranes were prepared by non-solvent vapour-induced phase separation (VIPS). The effects of bore fluid solution composition, coagulation bath temperature, air-gap distance and humidity on the morphologies of micro-porous PES hollow fibre membranes were investigated. Light transmission microscopy was used to determine the precipitation rate during VIPS stage as well as during non-solvent liquid-induced phase separation (LIPS) stage. The mean pore radius of PES hollow fibre UF membranes with sponge-like structures could be calculated by Image software from the SEM images. The mean pore radius of outer surface was about 0.1 μm (0.092 ~ 0.131 μm , PES3 ~ PES14) while the mean pore radius of the inner surface of PES hollow fibre membranes was 0.051-0.064 μm (PES12 and PES14). Pure water permeation fluxes and rejections were closely related to both the inner and outer skin layers. When inner and outer surfaces possessed open structure, the pure water permeation fluxes increased, whereas rejections decreased accordingly. PES hollow fibre membranes with pure water permeation flux from 387 to 1210 $\text{L}\cdot\text{m}^{-2}\cdot\text{h}^{-1}\cdot\text{bar}^{-1}$ as well as rejection of 10.1%-98.1% could be achieved by adjusting air humidity, air-gap distance and composition of bore fluid solution. Pure water permeation fluxes of PES12, PES13 and PES14 with sponge-like structures were higher than 1000 $\text{L}\cdot\text{m}^{-2}\cdot\text{h}^{-1}\cdot\text{bar}^{-1}$ and their BSA rejections were only about 10%.

Key Words:

surface pore size;
fabrication condition;
polyethersulphone;
hollow fibre membrane;
non-solvent vapour-induced phase separation.

INTRODUCTION

Generally, phase inversion is a process, in which techniques such as temperature and non-solvent induced phase separation (TIPS and NIPS) have been developed. Initially, in these techniques a homogeneous polymer solution becomes thermodynamically unstable due to external effects, and phase separates into a continuous polymer-rich phase that surrounds

the dispersed polymer-lean droplets [1-3]. Actually there are different ways to induce demixing of a polymer solution by NIPS on the basis of non-solvent physical state, i.e. non-solvent liquid-induced phase separation (LIPS) and non-solvent vapour-induced phase separation (VIPS) [4], which are much less studied than TIPS and NIPS. These methods are

(*) To whom correspondence to be addressed.
E-mail: chemxuzl@ecust.edu.cn

commonly used in the preparation of polymeric membranes for a variety of applications [5]. Besides, hollow fibre membranes have higher surface area per volume and higher packing density. In the preparation process of hollow fibre membranes, when the dope acquires the final morphology the properties of membranes are affected by extrusion pressure, coagulation bath composition and temperature, air-gap distance, humidity, rolling speed, etc. [6-9]. At present, polysulphone (PSF), polyethersulphone (PES), polyacrylonitrile (PAN), polyvinyl alcohol (PVC) and polyvinylidene fluoride (PVDF) hollow fibre membranes are fabricated for industrial applications [10-12]. However, most membranes of these materials are commonly obtained by TIPS and NIPS method; while few papers report the preparation of PES hollow fibre membranes by VIPS method.

Moreover, hollow fibre membranes with single inner skin layer were prepared by controlling both the chemistry and phase separation delayed rate of the external coagulant, while the preparation of hollow fibre membranes with single outer skin layer is not the same [13]. Xu et al. [14] prepared PES hollow fibre UF membranes using the additives of small molecular alcohols. Their results showed that the additives could efficiently dominate the membrane morphology and property. Liu et al. [15] fabricated hollow fibre MF/UF membranes with high permeation flux using PEG 400 and water as additives. Li et al. [16] indicated that the increase of solvents in bore fluid solution caused macro-porous structure formation on the inner surface of hollow fibre membrane as well as the increase of permeation flux. When the additional solvents were beyond certain critical value, dense layer with closed structure were induced, where the membrane formation process was controlled by nucleation and growth. Jacobs et al. [17] used high concentration solvents as the first step coagulation bath. In this way, the coagulation of outside skin layer could be efficiently dominated and macro-porous hollow fibre membranes with whole transfixion finger-like structure were obtained. Li et al. [2] investigated the preparation of PES flat sheet membranes by immersion precipitation combined with VIPS using diethylene glycol (DEG) as non-solvent additive and

N,N-dimethylacetamide (DMAc) as solvent. When the mass ratio of DEG to DMAc was nearly one, the cross-section morphologies of PES flat sheet membranes were sponge-like structures.

In this study, non-solvent vapour-induced phase separation (VIPS) method was adopted to prepare micro-porous polyethersulphone (PES) hollow fibre membranes with full sponge-like structure using the dope of PES:DMAc:DEG 17:43:40 (wt%). Full sponge-like structure could provide excellent mechanical strength as well as permeation property, but it would be relatively more difficult to achieve it compared to finger-like structure. Light transmission microscopy was used to determine the precipitation rate during VIPS stage as well as during non-solvent liquid-induced phase separation (LIPS) stage. The effects of bore fluid solution composition, coagulation bath temperature, air-gap distance and air humidity on the morphologies, the mean pore radius and other performances of PES hollow fibre UF membranes were investigated.

EXPERIMENTAL

Materials

The membrane-forming polymer, polyethersulphone (PES) (characteristic viscosity, $\eta = 0.48 \text{ dL.g}^{-1}$, density = 1.370 g.cm^{-3}) was produced by Jilin Jida High Performance Materials Co. Ltd. (China). *N,N*-Dimethylacetamide (DMAc) was purchased from Shanghai Xiang-Yang Chemical Reagent Corporation (China). Diethylene glycol (DEG) was purchased from Shanghai Lingfeng Chemical Reagent Corporation (China). Bovine serum albumin (BSA) ($\bar{M}_w = 67,000$) was purchased from Shanghai Bio Life Sci and Tech Co. Ltd. (China). De-ionized water was used throughout this work.

Light Transmittance Measurement

Light transmittance measurement experiments were carried out by a self-made device as described in literature [2,18,19]. A collimated laser was directed on the glass plate immersed in a non-solvent coagulation bath or exposed to air. The light intensity information was captured by a light detector and then recorded on a computer. The precipitation rate of the

dope could be characterized by the curve of light transmittance versus immersion time.

Preparation of Micro-porous PES Hollow Fibre Membranes

PES was dried at 90°C oven for 24 h before use. DMAc (solvent) and DEG (non-solvent) were mixed uniformly at first and then PES (polymer) was dissolved in the mixed solvent at 20°C. The composition of the membrane dope was as follows: 17 wt% PES/43 wt% DMAc/40 wt% DEG. Hollow fibre membrane spinning equipment was self-made [18,19]. The membrane dope was degassed at 20°C for at least 24 h to remove air bubbles. The membrane dope and coagulation bath (de-ionized water) were exchanged with solvent and non-solvent to form hollow fibre membranes. Nitrogen gas of 0.1 MPa pressure was introduced through the dope. The bore fluid rate was adjusted to make sure the ratio of inner/outer diameter of the hollow fibres was about 0.6, which was 1.0-1.3 mL/min. The rolling speed was the same with hollow fibre spinning rate, to avoid the tension effect on the membranes. The detailed fabrication conditions are summarized in Table 1. The fabricated hollow fibre membranes were stored in de-ionized water for at least 48 h to remove the residual solvents.

Preparation of Micro-porous PES Hollow Fibre Membranes Module

Membrane modules were prepared to test the hollow fibre separation performances quantitatively in terms of permeation flux and rejection. The outside-in feeding hollow fibre UF membrane modules with 22.5 cm length were self-prepared as described in literature [18,19]. The shell sides of the two ends of the bundles were glued onto two stainless steel tees using a normal-setting epoxy resin. These modules were left overnight in a 50 wt% glycerol water solution to be cured before tested. As it is known, post-treatment with glycerol solution to prevent the structural damage during handling is a general operation in membrane preparation. To eliminate the effect of the residual glycerol on module performance, each module was immersed in water for about 24 h.

Permeation Flux and Rejection of Micro-porous PES Hollow Fibre Membranes

The permeation flux and rejection of PES hollow fibre membranes testing equipment were employed according to methods described in literature [18,19]. All modules were run for 0.5 h under a pressure of 0.1 MPa before sample collection. An amount of 500 ppm BSA solution was used in membrane

Table 1. Spinning conditions of micro-porous PES hollow fibre membranes.

Membrane no.	Compositions of bore fluid solution (wt%)	Air-gap distance (cm)	Air humidity (%)	Temperature of coagulation bath (°C)
PES1	DMAc:H ₂ O = 0:100	0	-	25.0
PES2	DMAc:H ₂ O = 75:25	0	-	25.0
PES3	DMAc:H ₂ O = 0:100	10	60.0	25.0
PES4	DMAc:H ₂ O = 0:100	20	60.0	25.0
PES5	DMAc:H ₂ O = 0:100	30	60.0	25.0
PES6	DMAc:H ₂ O = 75:25	10	60.0	25.0
PES7	DMAc:H ₂ O = 75:25	20	60.0	25.0
PES8	DMAc:H ₂ O = 75:25	30	60.0	25.0
PES9	DMAc:H ₂ O = 0:100	10	60.0	40.0
PES10	DMAc:H ₂ O = 0:100	20	60.0	40.0
PES11	DMAc:H ₂ O = 0:100	30	60.0	40.0
PES12	DMAc:H ₂ O = 75:25	10	90.0	40.0
PES13	DMAc:H ₂ O = 75:25	20	90.0	40.0
PES14	DMAc:H ₂ O = 75:25	30	90.0	40.0

rejection testing. The concentrations of BSA in the infiltration and feed were determined by a UV-spectrophotometer (Shimadzu UV-3000, Japan). The pure water permeation flux (PWP) and rejection (R) were obtained by the formulae (1) and (2), respectively.

$$PWP = \frac{Q}{A \times T} \quad (1)$$

$$R = \left(1 - \frac{C_P}{C_F} \right) \times 100\% \quad (2)$$

where PWP is the pure water permeation flux of membranes or BSA solution ($L \cdot h^{-1} \cdot m^{-2}$), Q is the volume of the permeated pure water or BSA solution (L), A is the effective area of the membrane (m^2) and T is the permeation time (h). R is the rejection to BSA (%), C_P and C_F are permeate and feed concentrations, respectively (wt%).

Morphology of Micro-porous PES Hollow Fibre Membrane

The morphology of micro-porous PES hollow fibre membranes was examined by scanning electron microscopy (SEM) (Jeol Model JSM-6360 LV, Japan). The hollow fibre membranes were first immersed into liquid nitrogen for a few minutes, then broken and deposited on a copper holder. All samples were coated with gold in vacuum before test.

Pore Size Measurement of Micro-porous PES Hollow Fibre Membrane

Because of various conditions imposed on formation of inner and outer surfaces of hollow fibre membranes, surfaces with different pore densities were resulted in most cases. The mean pore radius, r_s , of the surface was determined by filtration velocity method which would lead to errors due to the non-uniformity of membrane walls. Because a sponge-like wall structure was obtained in the prepared hollow fibre membranes, their differences were mainly appeared on the surfaces as shown in SEM images. Moreover, the pure water flux as well as separation performance are not only determined by surface pore size alone but the porosity and interconnectivity may affect them as well. However,

because of the same membrane dope being adopted in this work, the porosity and interconnectivity in the membrane wall might be less effective than the membrane surfaces. Therefore, a SEM image analysis method was adopted to calculate surface mean pore radius of hollow fibre membranes. This could be realized by the counting function of software Image ProPlus 6.0. Hollow fibre membranes, with visible micro-pores on inner and outer surfaces from SEM images, could be statistically calculated by software Image ProPlus 6.0. The surface mean pore radius (r_s) and standard deviation, σ , are defined as following:

$$r_s = \frac{\sum_{t=1}^n r_t}{n} \quad (3)$$

$$s = \sqrt{\frac{\sum_{t=1}^n (r_t - r_s)^2}{n-1}} \quad (4)$$

RESULTS AND DISCUSSION

Precipitation Kinetics of PES Membrane Dopes

The precipitation kinetics of PES/DMAc/DEG system has been already discussed in previous work [2], which is mainly focused on the effect of additives concentrations on the precipitation kinetics. In this

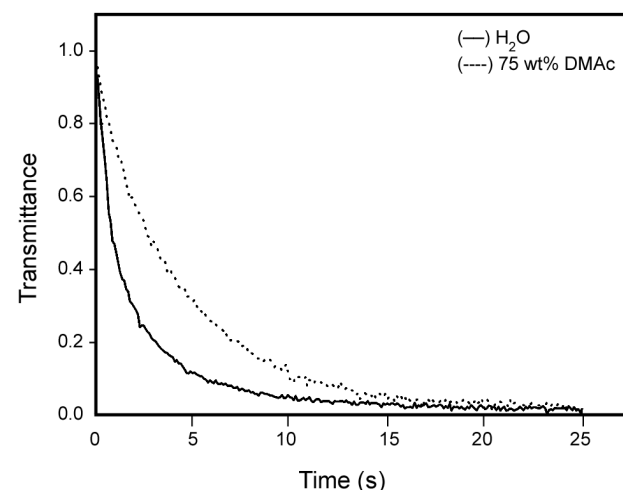


Figure 1. Light transmittance curves obtained by immersing dopes in different coagulation baths.

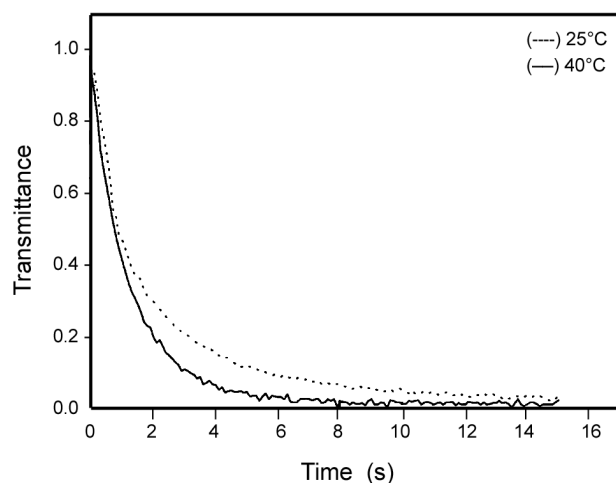


Figure 2. Light transmittance curves obtained by immersing dopes in coagulation baths with different temperatures.

case the effect of bore fluid solution composition, coagulation temperature and air humidity on PES membrane dope precipitation kinetics were emphasized. With air-gap distance of 10 cm, two compositions of without and with DMAc solutions (DMAc:H₂O = 0:100; 75 wt% DMAc with DMAc:H₂O = 75:25) were chosen as bore fluid solutions. As it is shown in Figure 1, in the precipitation rate of pure water (DMAc:H₂O = 0:100) as a coagulant it was much higher compared with DMAc:H₂O = 75:25 (75 wt% DMAc) as coagulant. The reason is that the addition of solvent (DMAc) into the coagulant decreases the deviation of solubility parameter values, and while a better miscibility is obtained the solvent diffusion rate is slowed down.

Based on previous work [2], the coagulation bath temperatures were selected as 25°C and 40°C. As it is shown in Figure 2, with an increase of coagulation bath temperature the diffusion between solvents and coagulant sharply accelerated. Therefore, the precipitation rate in the coagulation bath of 40°C water is much higher. Noticeably, there are two diffusion cases during hollow fibre membrane preparation process. Without air-gap distance, the solvent or non-solvent diffusion between polymer solution and bore fluid solution as well as that between solvent and coagulation bath takes place simultaneously. While with air-gap distance, the solvent or non-solvent diffusion between polymer solution and bore fluid solution takes place prior to that of solvent and

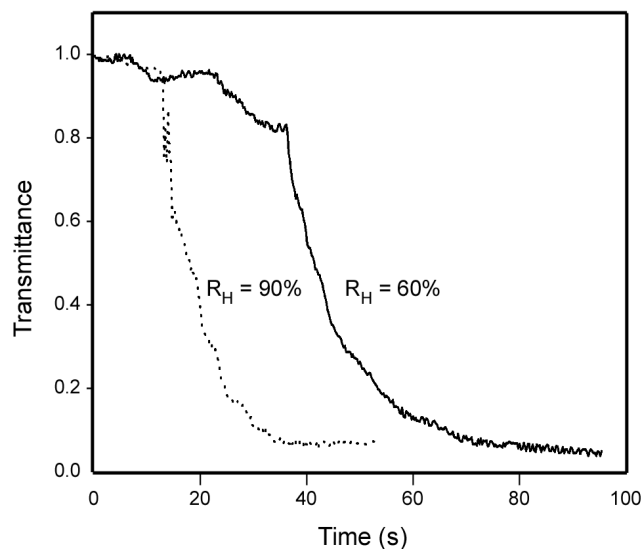


Figure 3. Light transmittance curves obtained by exposing dopes on air with different humidity percentages.

coagulation bath. The outward diffusion rate of non-solvent in bore fluid solution was quite high. When the air-gap distance is long enough, the membrane formation process is completed before hollow fibre membrane enters into the liquid-non-solvent coagulation bath. Therefore, the effect of coagulation bath temperature would be weakened.

The precipitation rates of the dope exposed in air with different degrees of humidity are shown in Figure 3. Higher precipitation rate is obtained in air with higher air humidity (R_H : 90%). This is because more water steam in air with higher humidity is transferred into the outer surface of polymer dope solution within the same time. Based on the conclusions derived in previous work [2], the membrane morphology was varied by different degrees of humidity. For middle humidity, the surface pore was mainly cellular, and it would be open interstices at high humidity.

Morphologies of Micro-porous PES Hollow Fibre Membranes

The cross-section morphologies of PES hollow fibre membranes under different fabrication conditions are shown in Figure 4. All cross-section morphologies of PES hollow fibre membranes are sponge-like structures. Bore fluid solution composition, coagulation bath temperature, air-gap distance and

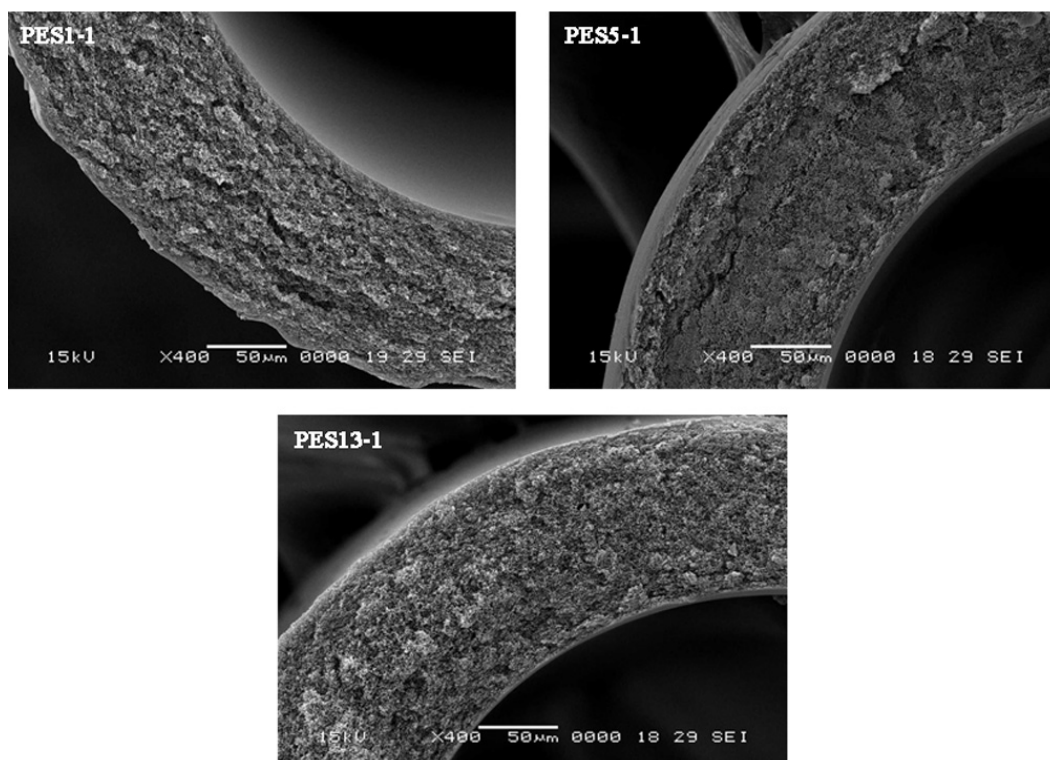


Figure 4. SEM Images of the cross-section of hollow fibre micro-porous PES membranes prepared under different spinning conditions (-1: cross-section, original magnification: 400×) with reference to Table 1.

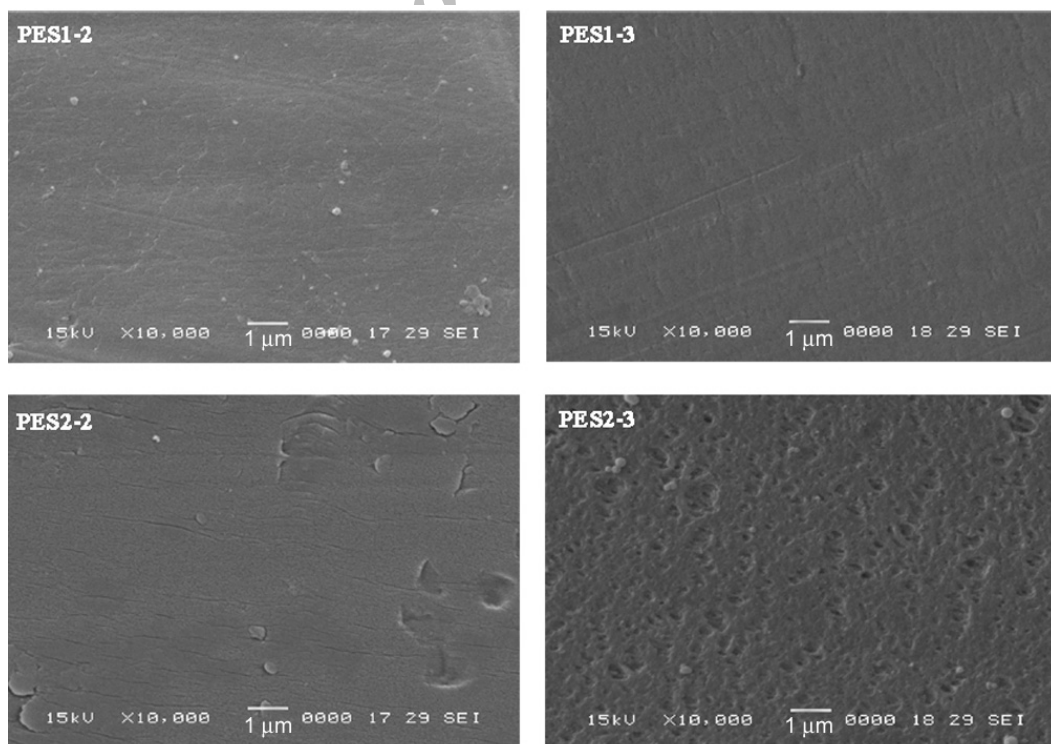


Figure 5. Effect of bore fluid composition on the surface morphology of micro-porous PES hollow fibre membranes (-2: outer surface, -3: inner surface; original magnification: 10000×) with reference to Table 1.

humidity do not obviously affect the cross-section morphologies of PES hollow fibre membranes in this work. This is due to the higher viscosity of polymer dope [PES:DMAc:DEG, 17:43:40 (wt%)] and in favour of sponge-like structure formation.

The effects of different bore fluid solutions on membrane surface without air-gap distance are shown in Figure 5. The outer surfaces of PES1-2 and PES2-2 are dense due to the instantaneous demixing. Dense

layers of PES1-3 also form on the inner surface due to instantaneous coagulation of the bore solution with pure water (DMAc:H₂O = 0:100). Because of the much weaker precipitation ability of the bore solution with DMAc:H₂O = 75:25 (wt%), a phase separation occurs which results in clear micro-porous structure on the inner surface as shown in PES2-3.

Figure 6 reveals the influence of air-gap distance on membrane surface morphology with two bore

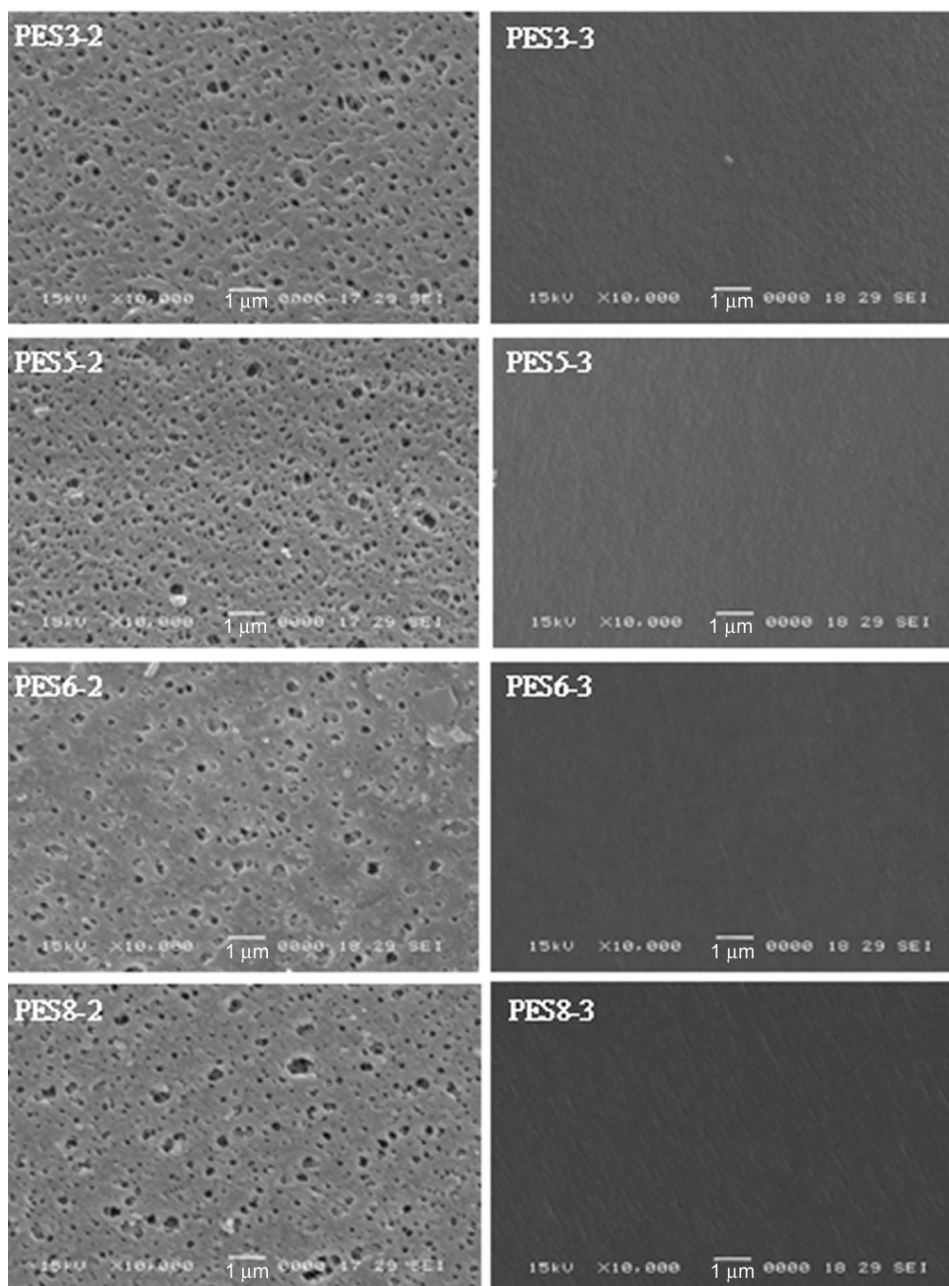


Figure 6. Effect of air-gap distance on the surface morphology of micro-porous PES hollow fibre membranes (-2: outer surface, -3: inner surface; original magnification: 10000 \times) with reference to Table 1.

fluid solutions (DMAc:H₂O = 0:100 and DMAc:H₂O = 75:25). There are no obvious differences on the inner surfaces of PES hollow fibre membranes. However the effect of air-gap distances on the outer surfaces of PES hollow fibre membranes for two bore fluid solutions are consistent. When air-gap distance is 10 cm, a clear micro-porous structure is found on the outer surface though air-gap distance is not long enough. When air-gap distance increases to 30 cm, the

numbers of micro-pores increase as well. This indicates that with the increase of air-gap distance the VIPS process of PES dope in air-gap distance is enhanced which results in the increased number of micro-pores. Because the increment of air-gap distance would allow the VIPS of membrane formation for a longer time, thus, it enhances the VIPS process. In the process of VIPS, a liquid-liquid phase separation would take place because of the thermal

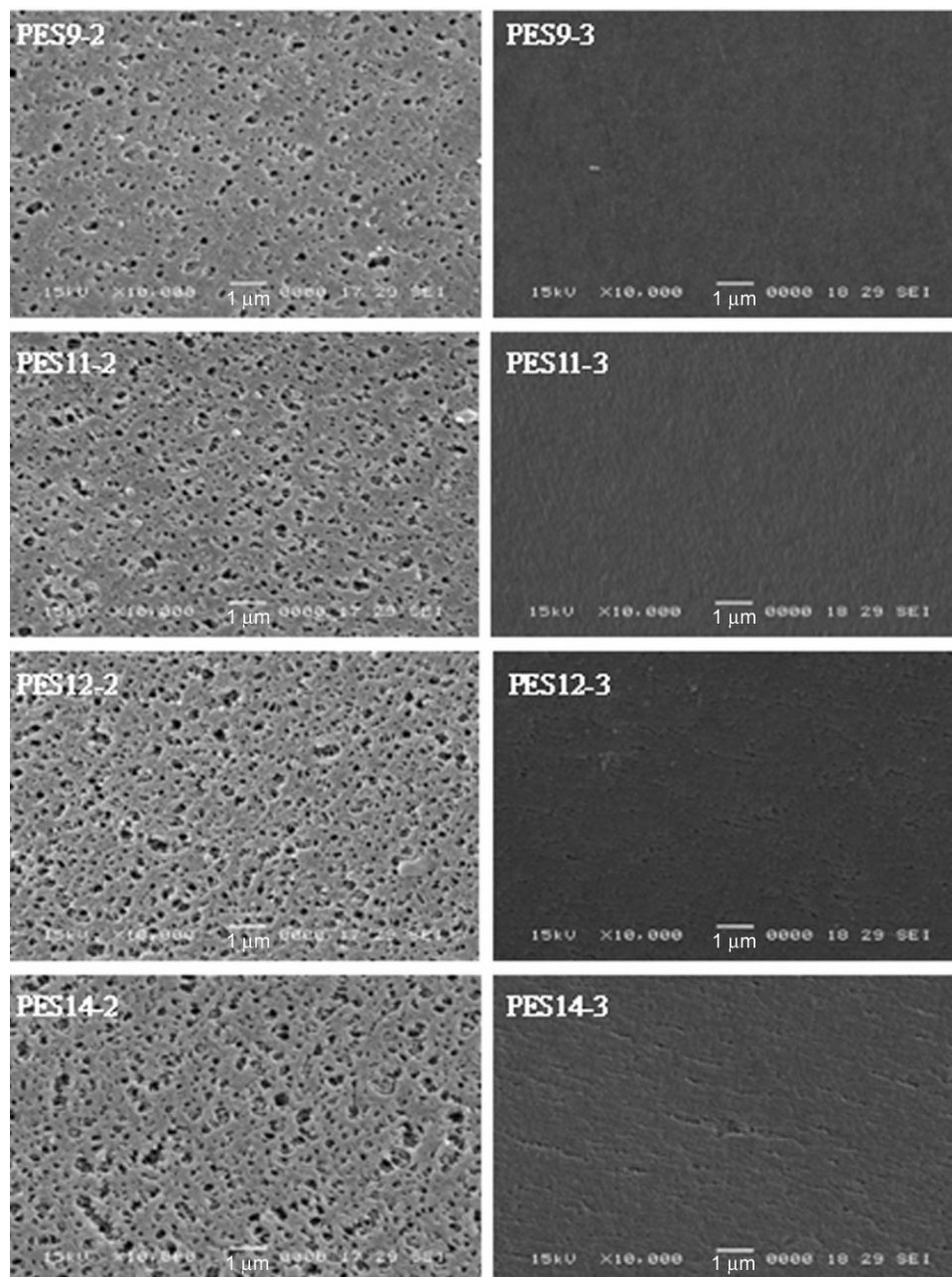


Figure 7. Effect of air humidity and coagulation bath temperature on the surface morphology of micro-porous PES hollow fibre membranes (-2: outer surface, -3: inner surface; original magnification: 10000 \times) with reference to Table 1.

instability. In this work, with the phase separation of DMAc and DEG, the porous structural formation is induced in the membranes

The effect of coagulation bath temperature and air humidity on membrane surface morphology is shown in Figure 7. Higher air humidity and coagulation bath temperature help micro-pores formation on membrane surface with the bore solution of DMAc:H₂O = 0:100 (wt%). The pore sizes on the outer surfaces of PES9 and PES11 are larger than those of PES3 and PES5. However, no obvious differences are found on the dense inner surfaces of PES9 and PES11. Visible micro-pores appear on both inner and outer surfaces of PES12 and PES14. However, micro-pores on the outer surfaces of PES12 and PES14 are larger in size and more obvious because of the VIPS process. Besides, on both inner and outer surfaces of PES hollow fibre membranes prepared at 90% air humidity, a better connectivity between the membrane layer and body is observed.

Although the spinning conditions have little effect on the cross-section morphologies, yet they change the surface morphologies of PES hollow fibre membranes. The formation of micro-porous structures on the outer surfaces of PES hollow fibre membranes are mainly determined by VIPS stage. Both air-gap distance and air humidity have stronger effect on the morphologies of the outer surfaces of PES hollow fibre membranes. Moreover, coagulation bath temperature would affect the pore sizes of PES hollow fibre membranes. The structures of inner surfaces are determined by bore fluid compositions. It is easy to understand that when air gap is zero, the inner surface of membrane is related to bore fluid. While with the air gaps of 10 cm and 30 cm, the VIPS process would be enhanced and a liquid-liquid separation would control the membrane structure, and thus the effect of bore fluid is weakened.

Surface Pore Sizes of Micro-porous PES Hollow Fibre Membranes

As it is shown in Table 2, the mean pore radius on the outer surfaces of PES hollow fibre membranes is about 0.1 μm (0.092~0.131 μm , PES3~PES14). With an increase of air-gap distance the surface mean pore radius increases slightly. Besides, the mean pore radius on the inner surfaces of PES hollow fibre

Table 2. Surface pore size analysis of inner and outer surfaces of micro-porous PES hollow fibre membrane.

Membrane no.	Pore in inner/outer surface	r_s (μm)
PES2	inner	0.086±0.003
PES3	outer	0.093±0.004
PES5	outer	0.098±0.004
PES6	outer	0.092±0.004
PES8	outer	0.095±0.005
PES9	outer	0.093±0.005
PES11	outer	0.111±0.006
PES12	outer	0.112±0.005
PES12	inner	0.051±0.003
PES14	outer	0.131±0.007
PES14	inner	0.064±0.003

membranes is 0.051~0.064 μm (PES12 and PES14). From the analysis of mean pore radius, both inner and outer surfaces of PES12-PES14 membranes possess micro-pore size as well as preferable permeation flux, which is in accordance with the characteristics of hollow fibre MF membranes.

Separation Performances of Micro-porous PES Hollow Fibre Membrane

Permeation fluxes and rejections of PES hollow fibre membranes are listed in Table 3. Pure water permeation flux (PWP) of PES1 without air-gap distance and with pure water as the bore fluid solution is 387 L.m⁻².h⁻¹ due to the dense structure of both inner and outer surfaces. On the contrary, pure water permeation fluxes of PES12, PES13 and PES14 are 1210 L.m⁻².h⁻¹, 1110 L.m⁻².h⁻¹ and 1090 L.m⁻².h⁻¹, respectively. This is due to visible micro-pores on both inner and outer surfaces of PES12, PES13 and PES14. Although higher coagulation bath temperature is adopted in the preparation of PES9, PES10 and PES11, pure water permeation fluxes of PES9, PES10 and PES11 are 574~610 L.m⁻².h⁻¹ and only about 50% pure water permeation fluxes of PES12, PES13 and PES14. It is illustrated that when pure water is used as bore fluid solution, the inner skin layers of PES9, PES10 and PES11 form dense layers due to the instantaneous demixing. However, by using DMAc:H₂O = 75:25 (wt%) as bore fluid solution, the

Table 3. Permeation and rejection properties of micro-porous PES hollow fibre membranes.

Membrane no.	Compositions of bore fluid solution (wt%)	Air-gap distance (cm)	Air humidity (%)	Coagulation bath temperature (°C)	PWP (L.m ⁻² .h ⁻¹)	R (%)
PES1	DMAc:H ₂ O = 0:100	0	-	25.0	387±19	98.1±0.12
PES2	DMAc:H ₂ O = 75:25	0	-	25.0	426±21	91.0±0.22
PES3	DMAc:H ₂ O = 0:100	10	60.0	25.0	703±32	92.9±0.17
PES4	DMAc:H ₂ O = 0:100	20	60.0	25.0	646±30	91.7±0.15
PES5	DMAc:H ₂ O = 0:100	30	60.0	25.0	666±35	92.1±0.20
PES6	DMAc:H ₂ O = 75:25	10	60.0	25.0	687±31	60.2±0.18
PES7	DMAc:H ₂ O = 75:25	20	60.0	25.0	663±29	59.8±0.11
PES8	DMAc:H ₂ O = 75:25	30	60.0	25.0	644±27	56.7±0.10
PES9	DMAc:H ₂ O = 0:100	10	60.0	40.0	610±28	85.0±0.12
PES10	DMAc:H ₂ O = 0:100	20	60.0	40.0	595±22	81.3±0.13
PES11	DMAc:H ₂ O = 0:100	30	60.0	40.0	574±21	82.6±0.19
PES12	DMAc:H ₂ O = 75:25	10	90.0	40.0	1210±40	12.3±0.12
PES13	DMAc:H ₂ O = 75:25	20	90.0	40.0	1110±39	10.8±0.10
PES14	DMAc:H ₂ O = 75:25	30	90.0	40.0	1090±35	10.1±0.10

inner skin layers of PES12, PES13 and PES14 form micro-porous layers due to the delayed demixing. As it is observed from Table 3, BSA rejection of PES1~PES14 could be varied between 10.1% and 98.1%. Besides, BSA rejection of PES1 is the highest rejection because of both inner and outer skin dense layers. While BSA rejection of PES2 with apparent opening structures on the inner surface is 91.0% due to its only dense outer skin layer. BSA rejections of PES12-PES14 with connective lacy pores on outer surfaces as well as micro-porous structures on the inner surfaces are the lowest of only about 10%.

Although, the pore density of inner and outer skin layers influences BSA rejections directly, either of inner and outer skin layers with dense structure would lead to higher rejection of micro-porous PES hollow fibre membranes. Therefore, the keys to fabricate PES hollow fibre membranes with sponge-like structures and single-skin layer are to control the chemistry/composition of bore-fluid solution, air humidity and polymer dope composition (given in this work). However, it is very important to point out that according to this work there is no critical molar volume for solvent of bore-fluid solution and critical polymer dope composition when preparing high-performance micro-porous PES hollow fibre membranes with sponge-like structures and single-skin layer.

CONCLUSION

Using a dope comprised of PES:*N,N*-dimethylacetamide (DMAc):diethylene glycol (DEG) 17:43:40 (wt%), micro-porous PES hollow fibre UF membranes with sponge-like structure were prepared by non-solvent vapour-induced phase separation (VIPS) method under different spinning conditions. The precipitation kinetics test indicated that bore fluid solution with 75% DMAc [DMAc:H₂O = 75:25 (wt%)] exhibited weaker ability for membrane formation compared to that of pure water [DMAc:H₂O = 0:100 (wt%)] for PES. With higher coagulation bath temperature and air humidity, higher precipitation rate was obtained. Cross-section morphologies of PES hollow fibre UF membranes show no obvious differences for the same polymer dope. The mean pore radius of outer surface was about 0.1 μm (0.092 ~ 0.131 μm, PES3 ~ PES14) while the mean surface pore radius on the inner surfaces of PES hollow fibre membranes is 0.051 ~ 0.064 μm (PES12 and PES14). Pure water permeation fluxes and rejections were closely related to the inner and skin layers. When inner and outer surfaces possessed opening structure, pure water permeation fluxes increased, whereas their rejection capabilities decreased correspondingly. PES hollow fibre UF membranes with pure water

permeation flux from 387 to 1210 L.m⁻².h⁻¹.bar⁻¹ as well as rejection of 10.1%-98.1% could be achieved by adjusting air humidity, air-gap distance and composition of bore fluid solution. Pure water permeation fluxes of PES12, PES13 and PES14 were higher than 1000 L.m⁻².h⁻¹.bar⁻¹ and their BSA rejections were only about 10%.

ACKNOWLEDGEMENT

The authors acknowledge the National Key Fundamental Research Development Plan ("973" Plan, No.2003CB615705) for giving financial supports in this project.

REFERENCES

- Li JF, Xu ZL, Yang H, Hydrophilic microporous PES membranes prepared by PES/PEG/DMAc casting solutions, *J Appl Polym Sci*, **107**, 4100-4108, 2008.
- Li JF, Xu ZL, Yang H, Microporous polyethersulfone membranes prepared under the combined precipitation conditions with non-solvent additives, *Polym Adv Technol*, **19**, 251-257, 2008.
- Bonyadi S, Chung TS, Krantz WB, Investigation of corrugation phenomenon in the inner contour of hollow fibers during the non-solvent induced phase-separation process, *J Membr Sci*, **299**, 200-210, 2007.
- Menut P, Su YS, Chinpa W, A top surface liquid layer during membrane formation using vapor-induced phase separation (VIPS)-evidence and mechanism of formation, *J Membr Sci*, **310**, 278-288, 2008.
- Yang XT, Xu ZL, Wei YM, Two-dimensional simulation of hollow fiber membrane fabricated by phase inversion method, *J Appl Polym Sci*, **100**, 2067-2074, 2006.
- Qusay FA, Xu ZL, Numerical simulation of a mathematical model for dry/wet-spun nascent hollow fiber membrane, *J Shanghai Univ*, **8**, 213-220, 2004.
- Chung TS, Xu ZL, Lin WH, Fundamental understanding of the effect of air-gap distance on the fabrication of hollow fiber membranes, *J Appl Polym Sci*, **72**, 379-395, 1999.
- Chung TS, Hu XD, Effect of air-gap distance on the morphology and thermal properties of polyethersulfone hollow fibers, *J Appl Polym Sci*, **66**, 1067-1077, 1997.
- Tsai HA, Kuo CY, Lin JH, Morphology control of polysulfone hollow fiber membranes via water vapor induced phase separation, *J Membr Sci*, **278**, 390-400, 2006.
- Yang Q, Chung TS, Santoso YE, Tailoring pore size and pore size distribution of kidney dialysis hollow fiber membranes via dual-bath coagulation approach, *J Membr Sci*, **290**, 153-163, 2007.
- Wijmans JG, Baaij JPB, Smolders CA, The mechanism of formation microporous or skinned membranes produced by immersion precipitation, *J Membr Sci*, **14**, 263-274, 1983.
- Yip Y, McHugh AJ, Modeling and simulation of non-solvent vapor-induced phase separation, *J Membr Sci*, **271**, 163-176, 2006.
- Yilmaz L, Mchugh AJ, Analysis of nonsolvent-solvent-polymer phase diagrams and their relevance to membrane formation modeling, *J Appl Polym Sci*, **31**, 997-1018, 1986.
- Xu ZL, Qusay FA, Effect of polyethylene glycol molecular weights and concentrations on polyethersulfone hollow fiber ultrafiltration membranes, *J Appl Polym Sci*, **91**, 3398-3407, 2004.
- Liu Y, Koops GH, Strathmann H, Characterization of morphology controlled polyethersulfone hollow fiber membranes by the addition of polyethylene glycol to the dope and bore liquid solution, *J Membr Sci*, **223**, 187-199, 2003.
- Li XM, He T, Does more solvent in bore liquid create more open inner surface in hollow fiber membranes, *Polym Adv Technol*, **19**, 801-806, 2008.
- Jacobs E P, Leukes WD, Formation of an externally unskinned polysulfone capillary membrane, *J Membr Sci*, **121**, 147-157, 1996.
- Lang WZ, Xu ZL, Yang H, Tong W, Preparation and characterization of PVDF-PFSA blend hollow fiber UF membrane, *J Membr Sci*, **288**, 123-131, 2007.
- Yuan GL, Xu ZL, Wei YM, Yu LY, Investigation on the morphologies and performances of PVDF-PFSA hollow fiber UF blend membranes, *Iran Polym J*, **18**, 891-902, 2009.